

*Original Research*

# Single-Cell RNA-Seq Reveals Changes in Cell Subsets in the Cortical Microenvironment during Acute Phase of Ischemic Stroke Rats

Yijin Zhao<sup>1,2,†</sup>, Chongwu Xiao<sup>1,†</sup>, Hui Chen<sup>1,†</sup>, Rui Zhu<sup>3</sup>, Meimei Zhang<sup>4</sup>, Haining Liu<sup>1</sup>, Xiaofeng Zhang<sup>1</sup>, Qing Zeng<sup>1,2,\*</sup>, Guozhi Huang<sup>1,2,\*</sup><sup>1</sup>Department of Rehabilitation Medicine, Zhujiang Hospital, Southern Medical University, 510280 Guangzhou, Guangdong, China<sup>2</sup>School of Rehabilitation Sciences, Southern Medical University, 528305 Foshan, Guangdong, China<sup>3</sup>Department of Oncology, First Affiliated Hospital of Gannan Medical University, 341000 Ganzhou, Jiangxi, China<sup>4</sup>Department of Rehabilitation, Affiliated Hospital of Jining Medical University, 272145 Jining, Shandong, China\*Correspondence: [zengqingyang@126.com](mailto:zengqingyang@126.com) (Qing Zeng); [drhuang66@163.com](mailto:drhuang66@163.com) (Guozhi Huang)

†These authors contributed equally.

Academic Editor: Gernot Riedel

Submitted: 21 December 2022 Revised: 19 March 2023 Accepted: 29 March 2023 Published: 22 August 2023

## Abstract

**Background:** Ischemic stroke, the most common stroke type, has threatened human life and health. Currently, intravenous thrombolysis and endovascular thrombectomy are the mainstream treatment methods, but they may cause cerebral ischemia-reperfusion injury (CIRI), which aggravates brain injury. Consequently, it is worthwhile to start with a study of CIRI mechanism to identify better prevention and treatment methods. Applying single-cell RNA sequencing (scRNA-seq) technology to further understand the biological functions of various cell types in CIRI will facilitate the intervention of CIRI. **Methods:** This study aimed to establish a rat middle cerebral artery occlusion (MCAO) model to simulate cerebral ischemia-reperfusion, perform enzymatic hydrolysis, and suspend cerebral cortex tissue edema. Single-cell transcriptome sequencing was used, combined with cluster analysis, t-distributed stochastic neighbor embedding (t-SNE) visualization, and other bioinformatics methods to distinguish cell subgroups while using gene ontology (GO) function enrichment and Kyoto encyclopedia of genes and genomes (KEGG) pathway enrichment to reveal the biological function of each cell subgroup. **Results:** We identified 21 brain clusters with cell type-specific gene expression patterns and cell subpopulations, as well as 42 marker genes representing different cell subpopulations. The number of cells in clusters 0–3 increased significantly in MCAO group compared to that in the sham group, and nine-cell subpopulations exhibited remarkable differences in the number of genes. Subsequently, GO and KEGG analyses were performed on the top 40 differentially expressed genes (DEGs) in the six cell subpopulations with significant differences. These results indicate that biological processes and signaling pathways are involved in different cell subpopulations. **Conclusions:** ScRNA-seq revealed the diversity of cell differentiation and the unique information of cell subpopulations in the cortex of rats with acute ischemic stroke, providing novel insight into the pathological process and drug discovery in stroke.

**Keywords:** ischemic stroke; cerebral ischemia-reperfusion injury; single-cell RNA-seq; MCAO; cellular heterogeneity

## 1. Introduction

Stroke, which has high morbidity, mortality, and disability rates, threatens human life and health while also imposing a significant economic burden on families and society [1]. A systematic analysis of the Global Burden of Disease Study 2019 indicates that stroke accounts for 11.6% of all deaths globally and remains the second leading cause of death [1]. Ischemic stroke accounts for approximately 80% of stroke patients [2]. Ischemic stroke is a neurological dysfunction caused by focal brain, spinal cord, or retinal infarction [3], including limb paralysis [4], spasm [5], dysphagia [6], aphasia [7], dysarthria [8], and depression [9]. Currently, ischemic stroke treatment mainly relies on intravenous thrombolysis and endovascular thrombectomy to achieve reperfusion of cerebral blood flow [10]. Although rapid blood flow reperfusion can effectively reduce brain cell death caused by ischemia, the resulting cerebral ischemia-reperfusion injury (CIRI) may trigger a series

of cascade events, such as necrotic apoptosis, free radical injury, and neuroinflammation, aggravating the damage to ischemic brain tissue and worsening patient prognosis [10–12]. Therefore, exploring better prevention and treatment methods based on the pathological mechanism of CIRI is the focus of ischemic stroke management.

Microglia and astrocytes are classified as M1/M2 or A1/A2 types, similar to macrophages [13–15]. An increasing number of studies indicate that this method of cell classification based on phenotypes and markers cannot reveal the complex cellular state in brain tissue after stroke. This may also be the main reason for almost all failures of interventions in immunomodulatory immune cells in the brain after stroke [16]. This highlights the importance of understanding the deleterious or beneficial effects of different immune cell subpopulations after stroke and the urgency of uncovering changes in cell subpopulations and key genes after stroke. Identifying cell subpopulations after



stroke is difficult because of their complex structure and diverse brain cell types. However, applying single-cell RNA-sequencing (scRNA-seq) technology has effectively alleviated this problem [17].

ScRNA-seq is a powerful tool for identifying individual cells [18–20]. We can rapidly determine the gene expression pattern of cells by measuring individual cell gene expression and analyzing the heterogeneity of genetic information within a cell subtype. Recently, scRNA-seq has been widely used in several fields to provide new insights into the heterogeneity of cell subpopulations in different tissues [17,21]. Therefore, this study aimed to reveal the heterogeneity and biological function of cell subpopulations in the cerebral cortex of acute ischemic rats by applying scRNA-seq, thereby providing a novel scheme and theoretical basis for the prevention and treatment of ischemic stroke.

## 2. Materials and Methods

### 2.1 Experimental Animals and Groups

The experimental animal protocol was approved by the Animal Experiment Ethics Committee of Zhujiang Hospital of Southern Medical University (LAEC-2020-235) and was carried out following the regulations of experimental animal management of Zhujiang Hospital of Southern Medical University. Specific pathogen-free (SPF) healthy male Sprague Dawley (SD) rats (weighing 280–300 g and 6–8 weeks old) were provided by the Laboratory Animal Center of Southern Medical University (license number: SCXK (Guangdong) 2016-0041). The rats were fed and drank water ad libitum. They were raised in an environment with a temperature of  $24 \pm 1$  °C,  $40 \pm 5\%$  humidity, and a 12 h light-dark cycle. Six rats were randomly divided into the Sham and middle cerebral artery occlusion (MCAO) groups, with three in each.

### 2.2 Establishment of Rat Models of Cerebral Ischemia-Reperfusion Injury

The rats were weighed and intraperitoneally injected with Avertin (0.2 mL/10 g, reagent center of Southern Medical University, Sigma-Aldrich, City of Saint Louis, MO, USA) [22]. After anesthesia, the rats were subjected to MCAO according to the method described by Longa [23]. Briefly, after exposing the common carotid artery (CCA), external carotid artery (ECA), and internal carotid artery (ICA) on the right side of the rat, a silicone-coated nylon monofilament (diameter, 0.3 mm) was inserted into ECA and passed through ICA until the middle cerebral artery was blocked. After ischemia for 1.5 h, the suture was slowly removed, and the wound was disinfected and sutured. The rats in the sham group were operated on according to the above procedure, but no sutures were inserted.

### 2.3 2, 3, 5-Triphenyl-2H-Tetrazolium Chloride Staining

Rats were randomly selected from each group 24 h after reperfusion for euthanasia [24]. After removing the brains, five 2-mm thick slices were serially transected in the brain matrix device. Brain slices were placed in a 2% 2, 3, 5-Triphenyl-2H-Tetrazolium Chloride (TTC) (T8877, Sigma-Aldrich, Riverdale, NJ, USA) solution and incubated at 37 °C for 15 min in the dark. Finally, sections were photographed, with red representing normal brain tissue and white representing infarcted areas.

### 2.4 Preparation of Single-Cell Samples from Rat Cortex

Rats in Sham and MCAO groups were euthanized, and their brains were removed to obtain cerebral cortical cells for scRNA-seq. One brain tissue specimen meeting the study requirements was selected from each group. The isolated cerebral cortex was prepared as a single-cell suspension. After gently mixing 10  $\mu$ L of the cell suspension and 10  $\mu$ L of 0.4% Trypan Blue Stain (T10282, Thermo Fisher Scientific, Waltham, MA, USA), 10  $\mu$ L of the mixture was quickly added to Countess® II Cell Counting. Cells were counted using a Countess® II Automated Cell Counter (C10228, Thermo Fisher Scientific, Waltham, MA, USA). The cell concentration in sham group was  $1.65 \times 10^6$  cells/ $\mu$ L, and 86% were living cells, while the cell concentration in MCAO group was  $1.43 \times 10^6$  cells/ $\mu$ L and 88% were living cells. If the proportion of viable cells was greater than 80%, it was considered a qualified sample, and subsequent experiments were performed after adjusting the cell concentration to 1000 cells/ $\mu$ L.

### 2.5 Single-Cell RNA Sequencing

Single-cell samples of rat cerebral cortex were sequenced using BD Rhapsody Single Cell Analysis System (Becton, Dickinson and Company, Lake Franklin, NJ, USA) [25,26]. The prepared single-cell suspension was added to a 20W+ microwell honeycomb plate. Beads with a unique molecular identifier (UMI) and cell barcode in the microplate were combined with the cells to capture and identify single cells. Following cell capture, total RNA was extracted from each well and reverse-transcribed into cDNA. The constructed cDNA library was sequenced on the Illumina NovaSeq 6000 sequencing platform (Illumina Inc., San Diego, CA, USA) to obtain the sequencing data. A count of  $\geq 1$  indicated that the gene was expressed. After excluding the genes expressed in less than three cells in the sequencing results, unqualified cells were excluded according to the following requirements: (1) Cells with more than 6000 or less than 200 genes were removed. (2) Cells with a mitochondrial gene ratio greater than 10% were removed. (3) The cells were removed with a hemoglobin gene ratio of  $>0.1\%$ .

## 2.6 Bioinformatics Analysis

After processing the sequencing results, Wilcoxon algorithm was used to compare cell subpopulation differences among the samples. Differentially expressed genes (DEGs) with fold change (FC) >2 and  $p$ -value < 0.05 were obtained in cell subpopulations. The top 40 DEGs were selected for gene ontology (GO) and Kyoto encyclopedia of genes and genomes (KEGG) analysis to clarify the biological processes and functions of cell subpopulations, according to the order of  $p$ -value from small to large (Fig. 1).

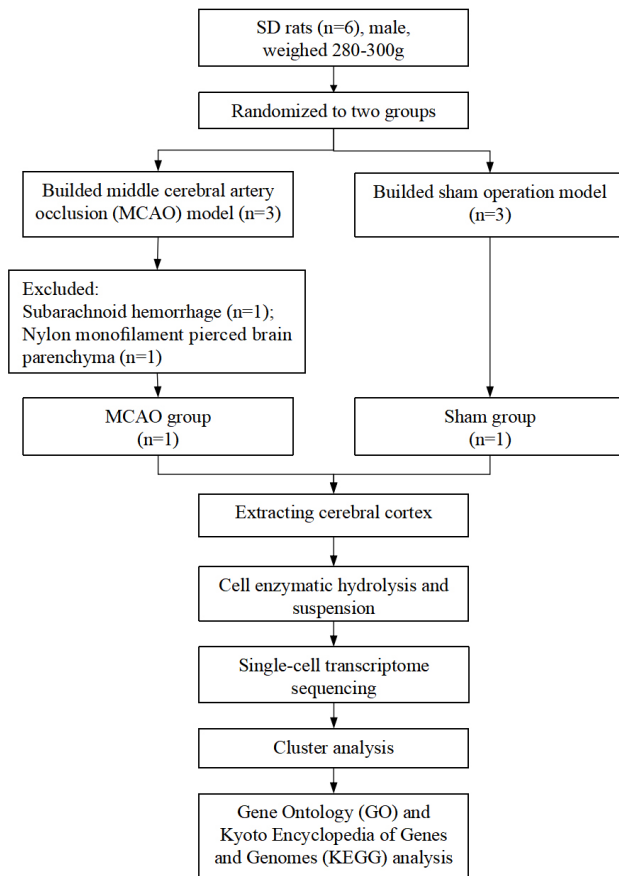


Fig. 1. Technology road map.

## 2.7 Statistical Analysis

DESeq2 package was used to determine the read counts of differentially expressed genes. The Student's two-tailed  $t$ -test was used to compare the two groups. All statistical analyses were performed using SPSS software (version 20.0, IBM Corp., Armonk, NY, USA), and figures were drawn using GraphPad Prism (version 5.0, GraphPad Software Company, San Diego, CA, USA) and Photoshop CC (version 2019, Adobe Systems Incorporated, San Jose, CA, USA). A  $p$ -value < 0.05 was defined as statistically significant.

## 3. Results

### 3.1 Preliminary Analysis of scRNA-seq Results

MCAO rat models were constructed and evaluated by TTC staining using scRNA-seq to detect changes in cell subpopulations in the cerebral cortex of acute ischemic rats. Fig. 2A displays that the cerebral infarction area of MCAO rat was white, and the normal tissue was red, indicating that MCAO rat model was successfully constructed. We then isolated the cortex of rats in the sham and MCAO groups and prepared cell suspensions for scRNA-seq (Fig. 2B). After sequencing, the results were preprocessed and normalized using Seurat R package. Unqualified cells were removed (Fig. 2B–D). The results demonstrated that 4,871 cells in the Sham group and 6,836 cells in MCAO group were identified by scRNA-seq (Fig. 2B–D). The filtered cells were subjected to cell cycle analysis. The cell cycle score of each cell was calculated according to the expression of the cell cycle genes to determine the cell cycle of each cell. Visual principal component analysis (PCA) data were used to evaluate cell cycle effects. If the cell cycle effect was excessive, a linear regression was used. The results indicated that the cell cycle effect was insignificant in this experiment, proving that the cell cycle effect had no significant effect on subsequent analysis (Fig. 2E–H).

### 3.2 Identification of Cell Subpopulations in Rat Cerebral Cortex with scRNA-seq

In this study, the brain cortex cells of sham and MCAO groups were identified using scRNA-seq based on BD Rhapsody system. After unbiased clustering analysis, the distribution of cells derived from the cerebral cortex of rats in sham and MCAO groups in each cell cluster was identified and visualized using t-distributed stochastic neighbor embedding (t-SNE) and Uniform Manifold Approximation and Projection (UMAP) dimensionality reduction algorithms, respectively (Fig. 3A,C). Subsequently, cell types were annotated using SingleR, and 21-cell clusters with unique gene expression patterns were defined (Fig. 3B,D). Fig. 3E depicts that although the number of cells and gene expression levels were different in each cell cluster in the two groups, the cell clusters were similar in the two groups. Notably, these 21-cell clusters were divided into 11 major cell lineages (Fig. 3F): microglia (clusters 0, 1, and 16), astrocytes (cluster 2), oligodendrocytes (clusters 3, 9, and 10), endothelial cells (clusters 4, 6, 11, 12, and 17), macrophages (cluster 5), ependymal cells (clusters 7 and 20), T cells (cluster 8), fibroblasts (clusters 13 and 19), monocytes (cluster 14), granulocytes/monocytes (cluster 15), and fibroblast activated (cluster 18). In conclusion, scRNA-seq data identified 21-cell clusters with high inter-cellular heterogeneity in the rat cortex.

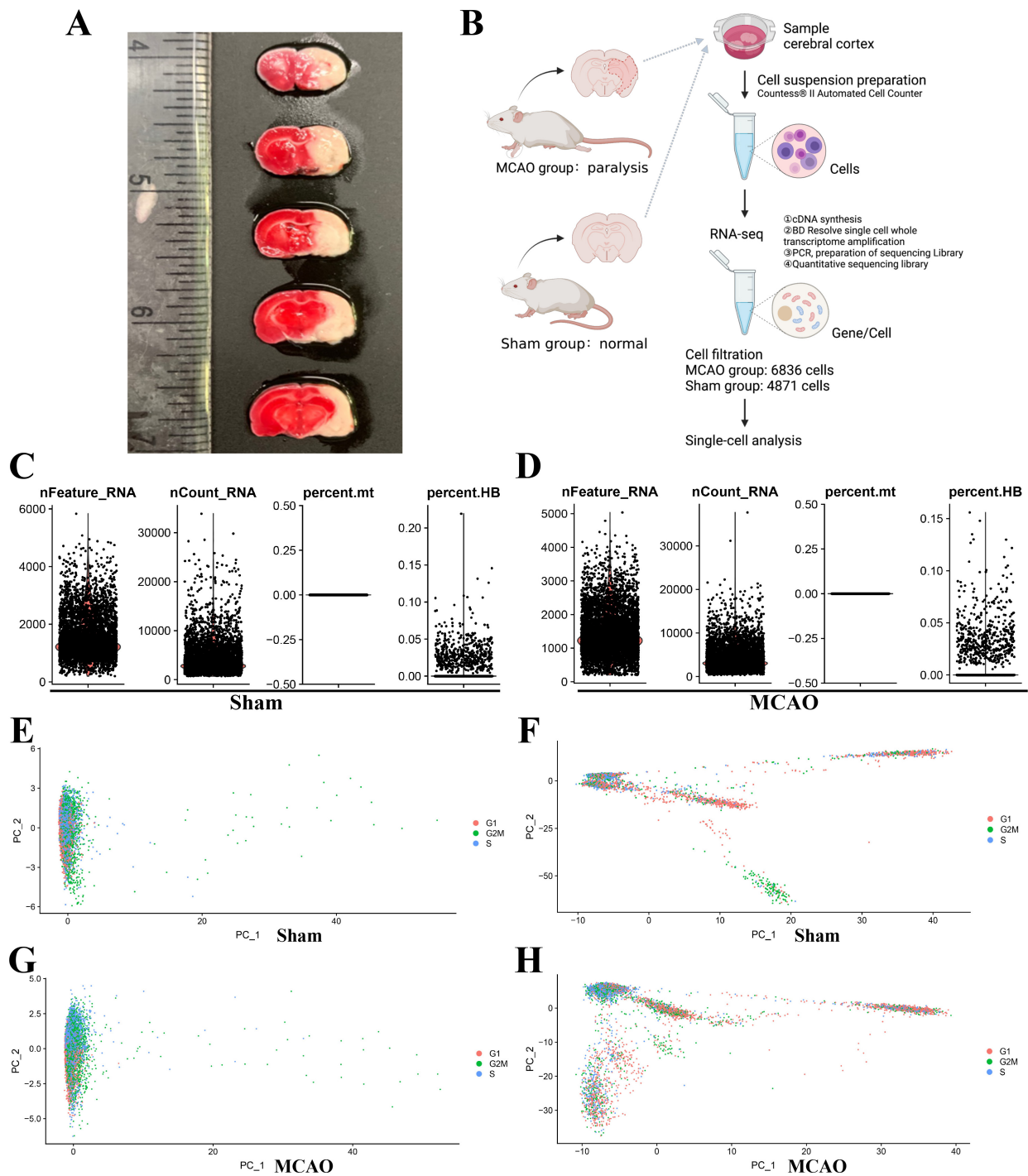


**Fig. 2. Experimental scheme and data preprocessing.** (A) 2, 3, 5-Triphenyl-2H-Tetrazolium Chloride (TTC) staining results after 24 h of middle cerebral artery occlusion (MCAO). The cerebral infarct area was stained white, and the normal tissue was red, indicating that the model was successfully established. (B) Schematic diagram of scRNA-seq workflow. (C) Violin diagram of the number of genes, the proportion of mitochondrial genes, and the proportion of hemoglobin genes in the samples of sham and (D) MCAO groups. (E,F) Principal component analysis (PCA) of cell cycle-related genes and all genes in the Sham group. (G,H) PCA of cell cycle-related genes and all genes in the MCAO group. In the PCA diagram, red dots represent cells in G1 phase, green dots represent cells in G2 or M phase, and blue dots represent cells in S phase.

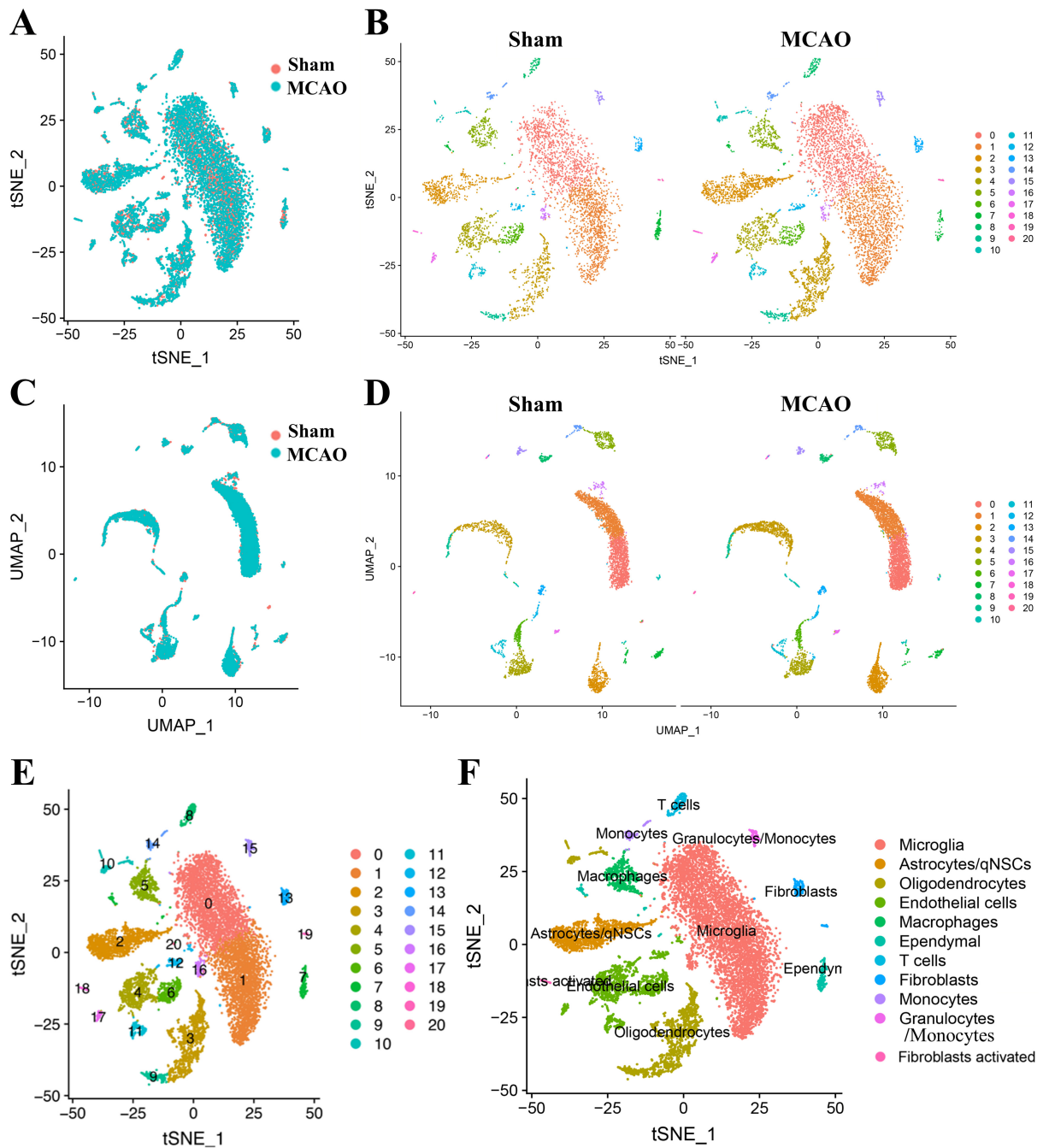


**Fig. 3.** Twenty-one cell clusters were identified in the sham and MCAO groups in the rat cortex. (A) t-distributed stochastic neighbor embedding (t-SNE) plot of cells in the sham and MCAO groups, where red dots represent cells derived from the sham group, and green dots display cells derived from MCAO group (n = 1). (B) t-SNE plot of 4871 cells in the sham group and the t-SNE plot of 6836 cells in MCAO group. The labels on the right were 21-cell clusters with corresponding colors, of which 0 to 20 represent microglia, microglia, astrocytes, oligodendrocytes, endothelial cells, macrophages, and endothelial cells, ependymal cells, T cells, oligodendrocytes, oligodendrocytes, endothelial cells, endothelial cells, fibroblasts, monocytes, granulocytes/monocytes, microglia, endothelial cells, activated fibroblasts, fibroblasts, and ependymal cells, respectively. (C) Uniform Manifold Approximation and Projection (UMAP) diagram of cells in the sham and MCAO groups, where red dots represent cells derived from the sham group, and green dots show cells derived from the MCAO group (n = 1). (D) Uniform Manifold Approximation and Projection (UMAP) diagram of 4871 cells in the sham group and Uniform Manifold Approximation and Projection (UMAP) diagram of 6836 cells in the MCAO group. (E) t-SNE plot of 21 cell clusters in the sham and MCAO groups. (F) t-SNE plot of 11 major cell lineages. t-SNE, t-distributed stochastic neighbor embedding.

**Table 1. The top two marker genes in each cell cluster.**

Cell cluster	Cell lineage	Marker genes
Cluster 0	Microglia	<i>Lyz2</i> and <i>Ccl4</i>
Cluster 1	Microglia	<i>Olr1</i> and <i>Bag3</i>
Cluster 2	Astrocytes	<i>Gjal</i> and <i>Gpr3711</i>
Cluster 3	Oligodendrocytes	<i>Mal</i> and <i>Plp1</i>
Cluster 4	Endothelial cells	<i>Cldn5</i> and <i>Flt1</i>
Cluster 5	Macrophages	<i>Cxcl1</i> and <i>Cxcl2</i>
Cluster 6	Endothelial cells	<i>Abcc9</i> and <i>Igfbp7</i>
Cluster 7	Ependymal cells	<i>Nnat</i> and <i>Terf2ip</i>
Cluster 8	T cells	<i>Cxcr4</i> and <i>Ccl5</i>
Cluster 9	Oligodendrocytes	<i>Ugt8</i> and <i>Apod</i>
Cluster 10	Oligodendrocytes	<i>Pdgfra</i> and <i>Vcan</i>
Cluster 11	Endothelial cells	<i>Hbb</i> and <i>Hba.a2</i>
Cluster 12	Endothelial cells	<i>Vin</i> and <i>Abcc9</i>
Cluster 13	Fibroblasts	<i>Tagln</i> and <i>Acta2</i>
Cluster 14	Monocytes	<i>RT1.Da</i> and <i>RT1.Ba</i>
Cluster 15	Granulocytes/monocytes	<i>S100a8</i> and <i>S100a9</i>
Cluster 16	Microglia	<i>RT1.Ba</i> and <i>Cd74</i>
Cluster 17	Endothelial cells	<i>Vwf</i> and <i>Mt2A</i>
Cluster 18	Fibroblasts activated	<i>Igf2</i> and <i>Col1a1</i>
Cluster 19	Fibroblasts	<i>Igfbp5</i> and <i>Ahcy12</i>
Cluster 20	Ependymal cells	<i>Folr1</i> and <i>Enpp2</i>

### 3.3 Identification and Analysis of Marker Genes of Different Cell Subpopulations in the Cerebral Cortex

We performed marker gene analysis of the 21-cell clusters to gain further insight into gene expression heterogeneity in each cell subpopulation in the MCAO rat cortex. The Wilcoxon rank-sum test was used to analyze genes in all cell clusters and then scored using One-vs-Res [27]. Genes with high specific expression,  $\log_{2}FC > 0.25$ , and expression in at least 20% of cells in each cell cluster were selected as significant marker genes of cell subpopulations. Subsequently, the top two marker genes in each cell cluster were drawn into a heatmap to display the marker gene expression in different cell clusters more intuitively (Fig. 4A). Fig. 4A depicts that each cell cluster was separated according to marker gene expression, indicating that the selected marker genes could accurately represent the cell clusters. The marker genes for each cell cluster are listed in Table 1. Additionally, t-SNE plots and violin plots of the marker genes of clusters 4, 6, 11, 12, and 17, with significant differences between sham and MCAO groups in the 21 cell clusters, were drawn to demonstrate the expression differences of the marker genes in the different cell clusters (Fig. 4B–K). In conclusion, 42 marker genes were identified in the rat cortex, elucidating gene expression heterogeneity in each cell subpopulation.

### 3.4 Changes of Cell Subpopulations in Rat Cerebral Cortex after MCAO

The number of cells in each cell cluster was analyzed in the cortex of rats, and it was found that the number of cells in clusters 0–3 increased significantly after

MCAO (Fig. 5A). Moreover, the proportion of cells in clusters 0–3 increased dramatically after MCAO (Fig. 5B). The heatmap of the proportion of 21 cell clusters revealed that clusters 0–3 were significantly different in the sham and MCAO groups. Cluster 20, an ependymal cell subset, was not observed in MCAO group (Fig. 5C). These results indicated that microglia, astrocytes, and oligodendrocytes, especially microglia, proliferated in the rat cerebral cortex after MCAO. As the most abundant resident immune effector cells in the central nervous system (CNS), significant microglial proliferation demonstrates the importance of microglia-based immunomodulatory interventions in preventing and treating ischemic stroke. A comparison of the number of genes in each cell cluster between the sham and MCAO groups revealed a significant difference in nine cell subsets between the two groups (Fig. 5D), including clusters 1 (microglia), 2 (astrocytes), 3 (oligodendrocytes), 4 (endothelial cells), 5 (macrophages), 6 (endothelial cells), 7 (ependymal cells), 10 (oligodendrocytes), and 19 (fibroblasts).

### 3.5 GO Analysis Revealed the Biological Process of Significantly Changed Cell Subpopulations in the Cerebral Cortex after MCAO

We selected the top 40 DEGs with the smallest  $p$ -value in the cell subpopulations for GO analysis to elucidate the biological processes involved in the six cell subpopulations that changed significantly after MCAO. Our analysis revealed that the biological enrichment process of the top 40 DEGs in cluster 1 was primarily related to the stress response after hypoxia (Fig. 6A), while cluster 2 may maintain protein homeostasis after MCAO, mainly through autophagy (Fig. 6B). Cell clusters 3 and 6 displayed similar biological processes, such as small GTPase-mediated signal transduction (Fig. 6C,D). Cluster 7 may be related to synapse formation (Fig. 6E), whereas cluster 10 mainly involved cell proliferation (Fig. 6F). In conclusion, GO analysis demonstrated that the biological processes involved in cell subpopulations were significantly altered in the rat cerebral cortex following MCAO.

### 3.6 KEGG Analysis Revealed the Signaling Pathways of Significantly Changed Cell Subpopulations in the Cerebral Cortex after MCAO

In addition, to GO analysis, we performed KEGG analysis on the top 40 DEGs in the cell subpopulations that were significantly altered after MCAO to further indicate the involved signaling pathways. Fig. 7 illustrates that KEGG analysis revealed the signaling pathways involved in Clusters 1, 2, 3, 6, 7, and 10 after MCAO. Notably, GO analysis revealed that the stress response after hypoxia in cluster 1 may be related to the HIF-1 signaling pathway, while autophagy in cluster 2 may be related to the mTOR signaling pathway. In conclusion, KEGG analysis further clarified the signaling pathways involved in DEGs in the significantly altered cell subpopulations after MCAO.

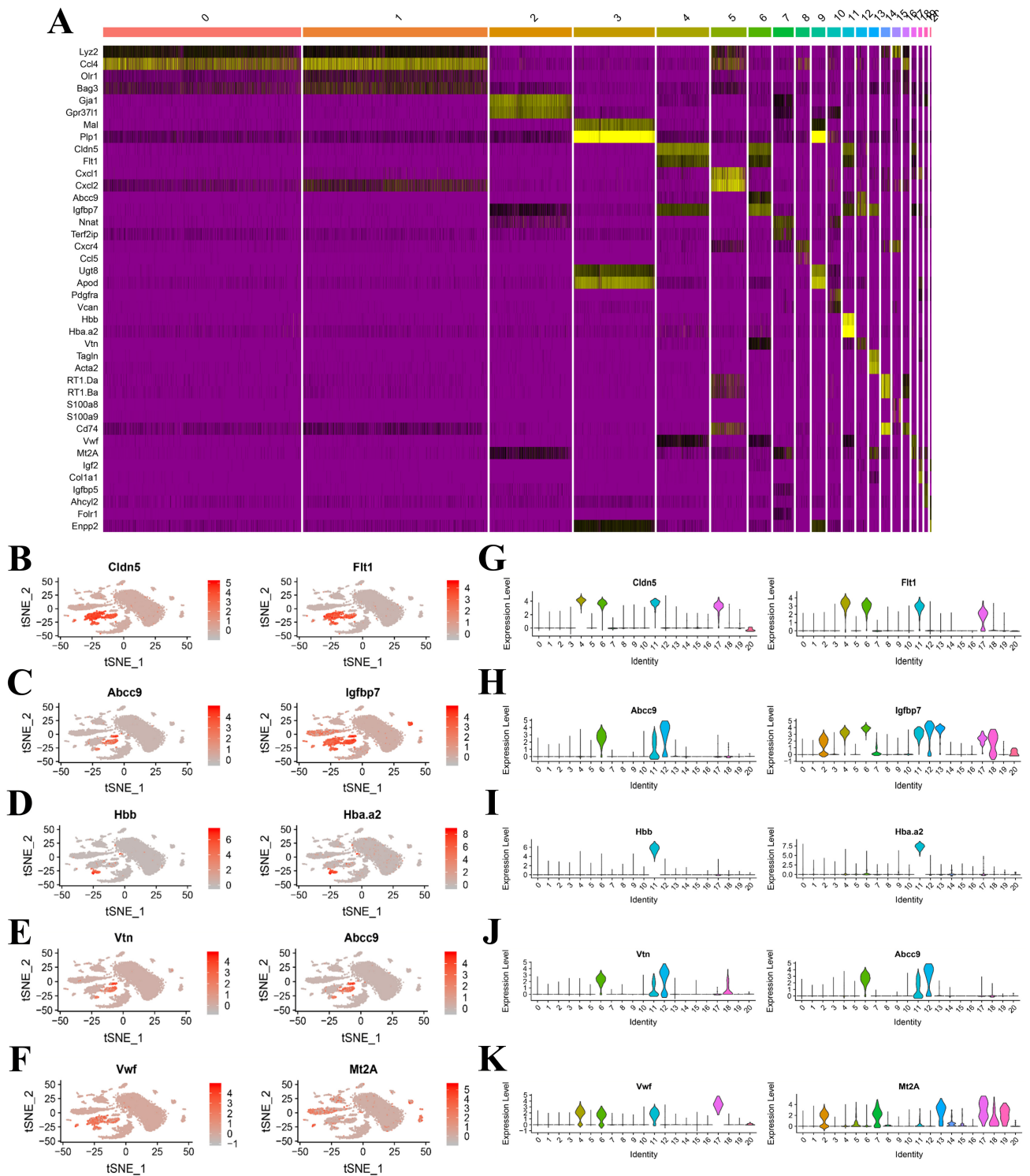


**Fig. 4. Identification of marker genes.** (A) Heatmap plots of the top two marker genes in each cell cluster. (B–F) The t-SNE plot depicted selected marker gene expression in clusters 4, 6, 11, 12, and 17. (G–K) Violin plots of selected marker gene expression of clusters 4, 6, 11, 12, and 17 in various cell clusters.

## 4. Discussion

The complexity of the central nervous system (CNS) is due to the existence of multiple cell types with specific gene expression patterns. Single-cell transcriptome sequencing

technology can accurately identify the different cell types in the central nervous system. Therefore, there is great potential to better understand cell types in the central nervous system.

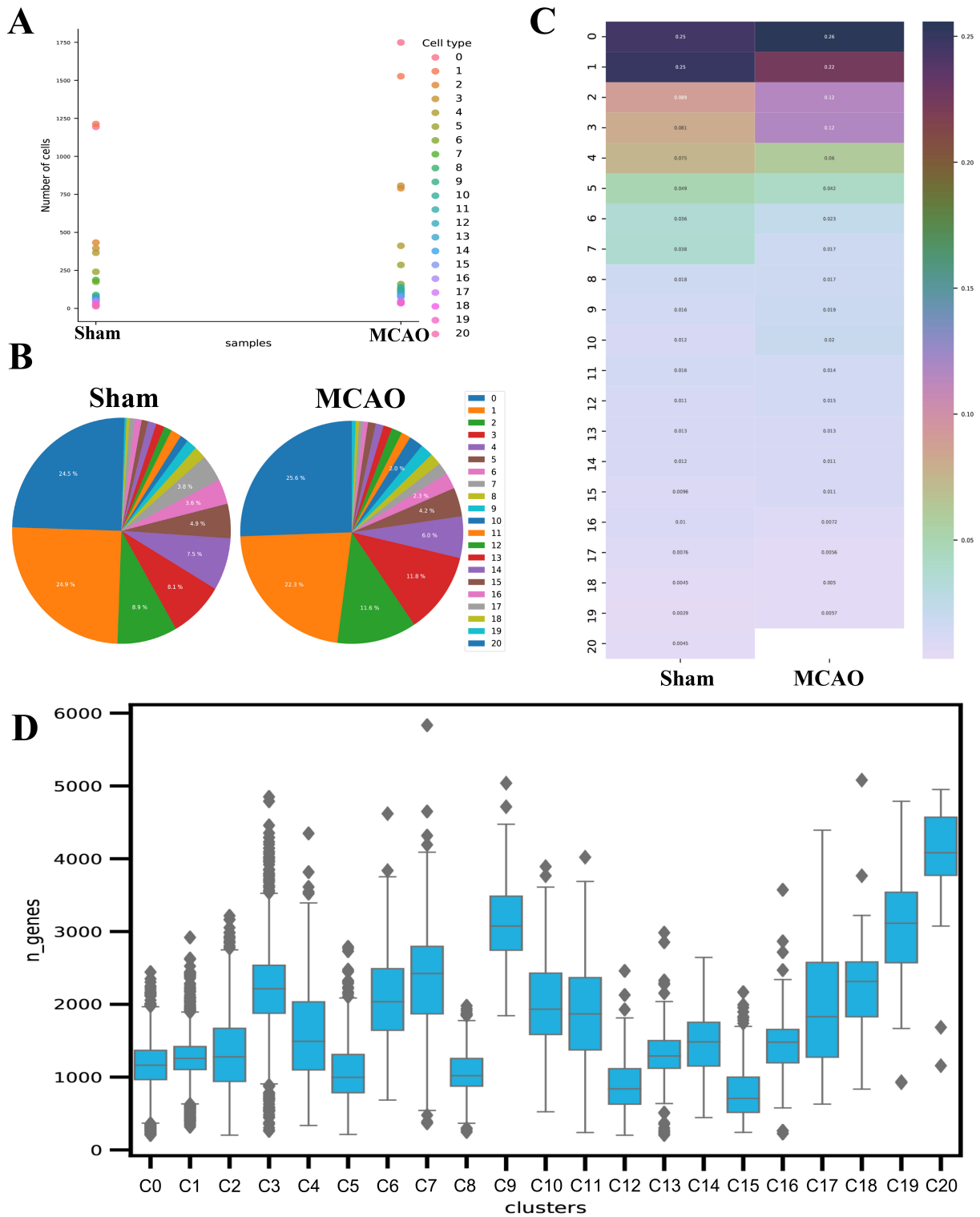


**Fig. 5. Analysis of differences between sham and MCAO groups.** (A) The number of cells per cluster in the sham and MCAO groups. (B) Pie charts depicting the cell proportion of each cell cluster in the sham and MCAO groups. (C) Heatmap presenting the cell proportion of each cell cluster in the sham and MCAO groups. (D) Gene numbers of cell clusters in rat cerebral cortex.

Although single-cell sequencing is still in its infancy compared to traditional sequencing technologies, such as genomics and conventional transcriptome sequencing, previous studies have demonstrated that single-cell RNA se-

quencing can be employed to identify different cell types in the central nervous system. Single-cell sequencing identified 39 cell subpopulations with different transcripts from the transcriptome of 44,808 mouse retinal cells, resulting in

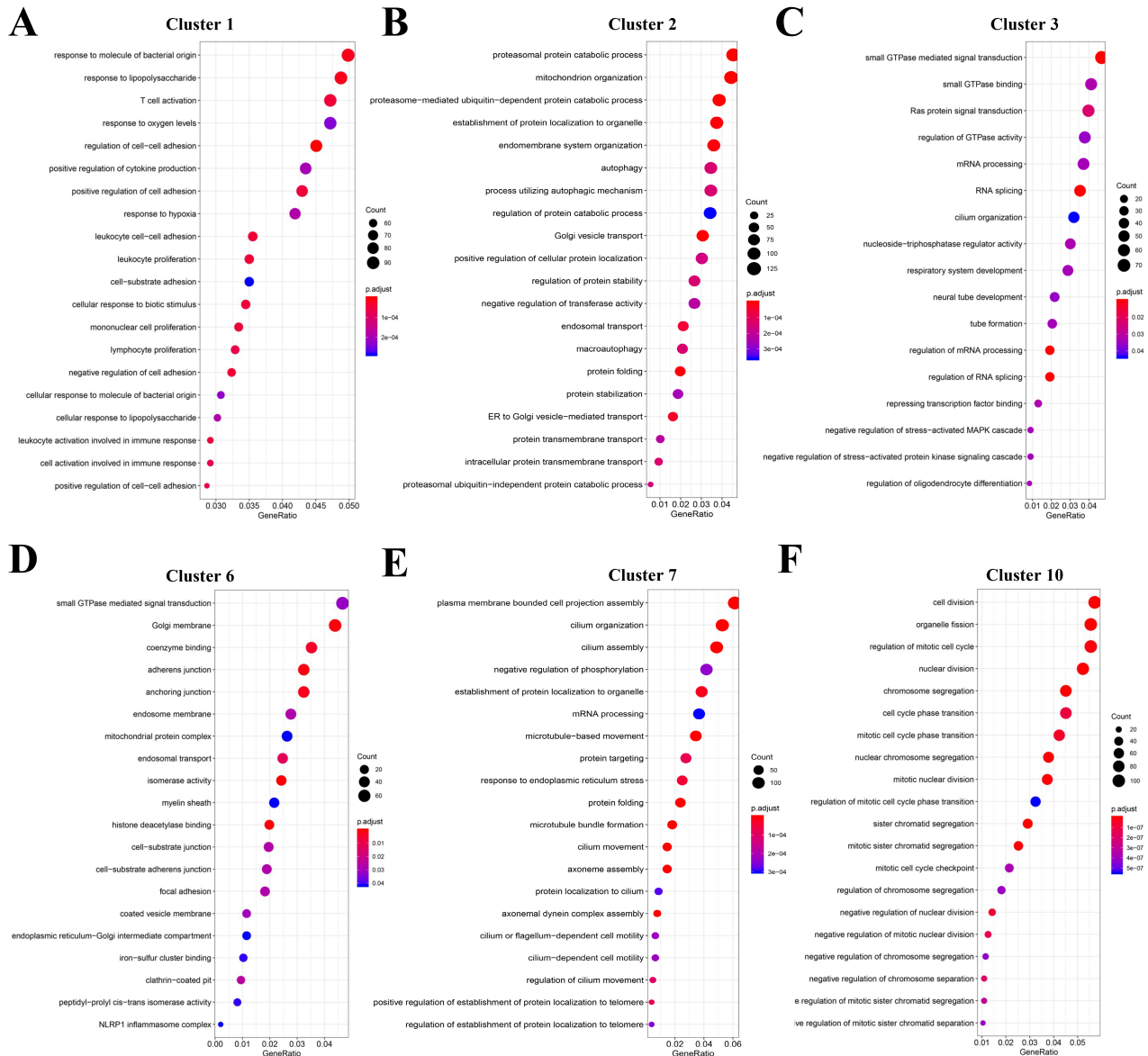


**Fig. 6. Go analysis of DEGs in cell subpopulations.** We performed GO analysis of DEG in cell clusters 1, 2, 3, 6, 7, and 10 to further clarify the biological function of significantly changed cell subsets after MCAO. (A) Bubble plot of GO analysis of the top 40 DEGs in cell cluster 1. (B) Bubble plot of GO analysis of the top 40 DEGs in cell cluster 2. (C) Bubble plot of GO analysis of the top 40 DEGs in cell cluster 3. (D) Bubble plot of GO analysis of the top 40 DEGs in cell cluster 6. (E) Bubble plot of GO analysis of the top 40 DEGs in cell cluster 7. (F) Bubble plot of GO analysis of the top 40 DEGs in cell cluster 10. The bubble size represents the number of DEGs enriched in the biological process, and the color represents the  $p$ -value. DEGs, differentially expressed genes; GO, gene ontology; KEGG, Kyoto encyclopedia of genes and genomes.

a molecular map of gene expression for known retinal and new candidate cell subtypes [28]. Similarly, another study analyzed the diversity of retinal bipolar cells via single-cell sequencing and identified 15 types of retinal bipolar cells, including all known and two novel cell subtypes [29]. Additionally, other researchers have revealed the diversity of cell types in the primary visual cortex of mice using single-cell sequencing techniques, including multiple nonneuronal cell subpopulations [30]. Meanwhile, the study discovered that

cell subpopulations with different transcriptomes exhibit specific and differential electrophysiological and axonal projection characteristics, suggesting that single-cell transcriptome signatures may be associated with specific cellular properties [30]. Therefore, in this experiment, the cell subpopulations in the cortical tissues of MCAO and normal rats were identified via scRNA-seq. The results identified 21 cell clusters, including cell cluster 0 (microglia), cell cluster 1 (microglia), cell cluster 2 (astrocytes/qNSCs),

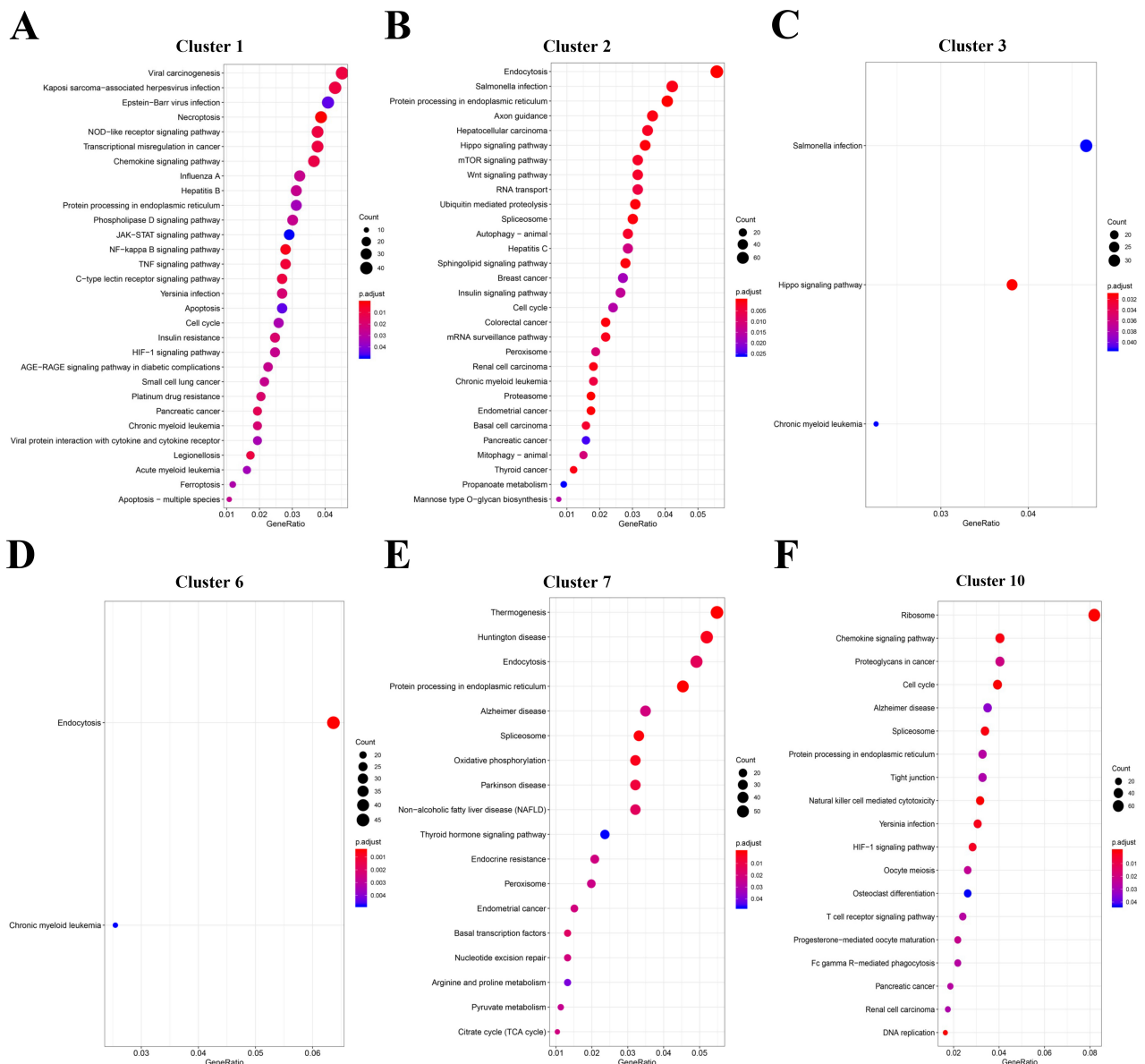


**Fig. 7. KEGG analysis of DEGs in cell subpopulations.** KEGG analysis was performed on DEGs in cell clusters 1, 2, 3, 6, 7, and 10. (A) Bubble plot of KEGG analysis of the top 40 DEGs in cell cluster 1. (B) Bubble plot of KEGG analysis of the top 40 DEGs in cell cluster 2. (C) Bubble plot of KEGG analysis of the top 40 DEGs in cell cluster 3. (D) Bubble plot of KEGG analysis of the top 40 DEGs in cell cluster 6. (E) Bubble plot of KEGG analysis of the top 40 DEGs in cell cluster 7. (F) Bubble plot of KEGG analysis of the top 40 DEGs in cell cluster 10. The bubble size represents the number of DEGs enriched in the biological process, and the color represents the *p*-value.

cell cluster 3 (oligodendrocytes), cell cluster 4 (endothelial cells), cell cluster 5 (macrophages), cell cluster 6 (endothelial cells), cell cluster 7 (ependymal), cell cluster 8 (T cells), cell cluster 9 (oligodendrocytes), cell cluster 10 (oligodendrocytes), cell cluster 11 (endothelial cells), cell cluster 12 (endothelial cells), cell cluster 13 (fibroblasts), cell cluster 14 (monocytes), cell cluster 15 (granulocytes/monocytes), cell cluster 16 (microglia), cell cluster 17 (endothelial cells), cell cluster 18 (fibroblasts activated), cell cluster 19 (fibroblasts), cell cluster 20 (ependymal).

The scRNA-seq technology can distinguish between different cell types and subtypes. In this experiment, we discovered that the same cell type clustered into different cell subgroups. Microglia are divided into three subpopulations, oligodendrocytes into three subpopulations, endothelial cells into five subpopulations, and ependymal cells and fibroblasts into two subpopulations. Simultaneously, we noticed that microglia had the highest number of cells after MCAO, which is consistent with previous studies [2,31,32]. When cerebral ischemia occurs, glial cells are

activated first, especially microglia [2]. However, whether microglia have significant polarization within 24 h of cerebral ischemia-reperfusion remains controversial [33]. Our scRNA-seq data revealed that microglia differentiated into three cell subtypes, cell clusters 0, 1, and 16, at 24 h after MCAO. This differs from traditional cognition. Previous studies have divided microglia into M1 and M2 types [34]. In this experiment, we discovered a third type of microglia, which may represent an intermediate transition body in the transition process of M1 and M2 microglia. Microglia, as a “double-edged sword”, promote neuroinflammation or injury repair in stroke development [35]. Previous studies have revealed that inflammation is associated with aortic stiffening [36], and our findings suggest that inflammation is associated with cerebrovascular sclerosis, given their high degree of uniformity. Therefore, there is an urgent need to inhibit the polarization of microglia to the pro-inflammatory type and drive their polarization to the protective type during the acute phase of ischemic stroke. Our sequencing results provided important information for identifying therapeutic targets for ischemic stroke and characterizing early cell changes by mining the heterogeneity of cell types in the rat cerebral cortex.

In this study, we found that the microenvironment of rat cortical tissue changed compared to the gene expression of different cell subpopulations in normal cortical tissue after MCAO, which was mainly reflected in nine cell subpopulations: cell cluster 0 (microglia), cell cluster 1 (microglia), cell cluster 2 (astrocytes/qNSCs), cell cluster 3 (oligodendrocytes), cell cluster 4 (endothelial cells), cell cluster 5 (macrophages), cell cluster 6 (endothelial cells), cell cluster 7 (ependymal), cell cluster 10 (oligodendrocytes), and cell cluster 19 (fibroblasts). Moreover, the Wilcoxon algorithm revealed that cell clusters 1, 2, 3, 6, 7, and 10 exhibit statistically significant differences between the two samples. GO, and KEGG analyses of the top 40 DEGs in cell subpopulations with significant differences revealed that the participation of cluster 1 in the stress response after hypoxia may be related to the HIF-1 signaling pathway, whereas the autophagy involved in cluster 2 may be related to the mTOR signaling pathway. These pathways may be key regulators of microglia and astrocytes after MCAO and provide a new perspective for future research.

This study had some limitations. The first limitation concerns the experimental subjects. Although we simulated cerebral ischemia-reperfusion injury in rats, the brain microenvironment blueprint derived from experimental animal data does not perfectly represent that of humans. Second, our findings are based on scRNA-seq data and the low sample size due to the high scRNA-seq technology cost. Therefore, further verification was required.

## 5. Conclusions

In this study, 21-cell clusters were identified using scRNA-seq to detect the cerebral cortex of normal and MCAO rats, including three types of microglia, three types of oligodendrocytes, five types of endothelial cells, two types of ependymal cells, two types of fibroblasts, two types of monocytes, neurons, astrocytes, T-cells, and macrophages. Simultaneously, 42 marker genes were identified in different cell subsets. GO, and KEGG analyses of the top 40 DEGs in six cell subpopulations with significant differences revealed the biological processes and signaling pathways of different cell subsets. In conclusion, this study revealed the diversity of cortical cell differentiation and the unique information on cell subsets in rats with acute ischemic stroke, providing a new perspective for the study of the pathological process of ischemic stroke.

## Availability of Data and Materials

The datasets used and/or analyzed during the current study are available from the corresponding author on reasonable request.

## Author Contributions

GZH and QZ designed and supervised the study. YJZ, MMZ, HNL established the MCAO rat model and drew Fig. 1. YJZ, CWX, RZ, and HC analyzed the single-cell RNA sequencing results and prepared Figs. 2–7. CWX and XFZ for Statistical analysis. GZH and YJZ wrote the manuscript. All authors contributed to editorial changes in the manuscript. All authors read and approved the final manuscript. All authors have participated sufficiently in the work and agreed to be accountable for all aspects of the work.

## Ethics Approval and Consent to Participate

The experimental animal protocol was approved by the Laboratory Animal Ethics Committee, Zhujiang Hospital of SMU (LAEC-2020-235) and was carried out following the regulations of experimental animal management of Zhujiang Hospital of Southern Medical University. All animal experiments were performed in accordance with the guidelines of NIH.

## Acknowledgment

We would like to thank the staff in the central laboratory of Zhujiang Hospital and the laboratory of Heart Center, Southern Medical University. I sincerely appreciate the other members of our department, especially Yilei Zhang, and Chen Li, for their discussions and help. We also thank Shanghai Biotechnology Corporation (Shanghai, China) to help us in scRNA sequencing.

## Funding

This study was supported by the National Natural Science Foundation of China (82072528, 81874032, 82002380) and National Health Commission project of China (DCMST-NHC-2019-AHT-01).

## Conflict of Interest

The authors declare no conflict of interest. The authors state that the study was conducted in the absence of any business or financial relationships that could be construed as potential conflicts of interest.

## References

- [1] GBD 2019 Stroke Collaborators. Global, regional, and national burden of stroke and its risk factors, 1990-2019: a systematic analysis for the Global Burden of Disease Study 2019. *The Lancet. Neurology*. 2021; 20: 795–820.
- [2] Xu S, Lu J, Shao A, Zhang JH, Zhang J. Glial Cells: Role of the Immune Response in Ischemic Stroke. *Frontiers in Immunology*. 2020; 11: 294.
- [3] Sacco RL, Kasner SE, Broderick JP, Caplan LR, Connors JJB, Culebras A, *et al.* An updated definition of stroke for the 21st century: a statement for healthcare professionals from the American Heart Association/American Stroke Association. *Stroke*. 2013; 44: 2064–2089.
- [4] Hong Z, Sui M, Zhuang Z, Liu H, Zheng X, Cai C, *et al.* Effectiveness of Neuromuscular Electrical Stimulation on Lower Limbs of Patients With Hemiplegia After Chronic Stroke: A Systematic Review. *Archives of Physical Medicine and Rehabilitation*. 2018; 99: 1011–1022.e1.
- [5] Pundik S, McCabe J, Skelly M, Tatsuoka C, Daly JJ. Association of spasticity and motor dysfunction in chronic stroke. *Annals of Physical and Rehabilitation Medicine*. 2019; 62: 397–402.
- [6] Bath PM, Lee HS, Everton LF. Swallowing therapy for dysphagia in acute and subacute stroke. *The Cochrane Database of Systematic Reviews*. 2018; 10: CD000323.
- [7] Stefaniak JD, Halai AD, Lambon Ralph MA. The neural and neurocomputational bases of recovery from post-stroke aphasia. *Nature Reviews. Neurology*. 2020; 16: 43–55.
- [8] Chiamonte R, Pavone P, Vecchio M. Speech rehabilitation in dysarthria after stroke: a systematic review of the studies. *European Journal of Physical and Rehabilitation Medicine*. 2020; 56: 547–562.
- [9] Das J, G K R. Post stroke depression: The sequelae of cerebral stroke. *Neuroscience and Biobehavioral Reviews*. 2018; 90: 104–114.
- [10] Sun MS, Jin H, Sun X, Huang S, Zhang FL, Guo ZN, *et al.* Free Radical Damage in Ischemia-Reperfusion Injury: An Obstacle in Acute Ischemic Stroke after Revascularization Therapy. *Oxidative Medicine and Cellular Longevity*. 2018; 2018: 3804979.
- [11] Przykaza Ł. Understanding the Connection Between Common Stroke Comorbidities, Their Associated Inflammation, and the Course of the Cerebral Ischemia/Reperfusion Cascade. *Frontiers in Immunology*. 2021; 12: 782569.
- [12] Liao S, Apaijai N, Chattipakorn N, Chattipakorn SC. The possible roles of necroptosis during cerebral ischemia and ischemia / reperfusion injury. *Archives of Biochemistry and Biophysics*. 2020; 695: 108629.
- [13] Xiong XY, Liu L, Yang QW. Functions and mechanisms of microglia/macrophages in neuroinflammation and neurogenesis after stroke. *Progress in Neurobiology*. 2016; 142: 23–44.
- [14] Kanazawa M, Ninomiya I, Hatakeyama M, Takahashi T, Shimohata T. Microglia and Monocytes/Macrophages Polarization Reveal Novel Therapeutic Mechanism against Stroke. *International Journal of Molecular Sciences*. 2017; 18: 2135.
- [15] Liu LR, Liu JC, Bao JS, Bai QQ, Wang GQ. Interaction of Microglia and Astrocytes in the Neurovascular Unit. *Frontiers in Immunology*. 2020; 11: 1024.
- [16] Zera KA, Buckwalter MS. The Local and Peripheral Immune Responses to Stroke: Implications for Therapeutic Development. *Neurotherapeutics: the Journal of the American Society for Experimental Neurotherapeutics*. 2020; 17: 414–435.
- [17] Mickelsen LE, Bolisetty M, Chimileski BR, Fujita A, Beltrami EJ, Costanzo JT, *et al.* Single-cell transcriptomic analysis of the lateral hypothalamic area reveals molecularly distinct populations of inhibitory and excitatory neurons. *Nature Neuroscience*. 2019; 22: 642–656.
- [18] Shalek AK, Satija R, Adiconis X, Gertner RS, Gaublomme JT, Raychowdhury R, *et al.* Single-cell transcriptomics reveals bimodality in expression and splicing in immune cells. *Nature*. 2013; 498: 236–240.
- [19] Butler A, Hoffman P, Smibert P, Papalexi E, Satija R. Integrating single-cell transcriptomic data across different conditions, technologies, and species. *Nature Biotechnology*. 2018; 36: 411–420.
- [20] Yamada S, Nomura S. Review of Single-Cell RNA Sequencing in the Heart. *International Journal of Molecular Sciences*. 2020; 21: 8345.
- [21] Cohen M, Giladi A, Gorki AD, Solodkin DG, Zada M, Hladik A, *et al.* Lung Single-Cell Signaling Interaction Map Reveals Basophil Role in Macrophage Imprinting. *Cell*. 2018; 175: 1031–1044.e18.
- [22] Wang D, Chen L, Fu Y, Kang Q, Wang X, Ma X, *et al.* Avertin affects murine colitis by regulating neutrophils and macrophages. *International Immunopharmacology*. 2020; 80: 106153.
- [23] Longa EZ, Weinstein PR, Carlson S, Cummins R. Reversible middle cerebral artery occlusion without craniectomy in rats. *Stroke*. 1989; 20: 84–91.
- [24] Hawkins P, Prescott MJ, Carbone L, Dennison N, Johnson C, Makowska IJ, *et al.* A Good Death? Report of the Second Newcastle Meeting on Laboratory Animal Euthanasia. *Animals: an Open Access Journal from MDPI*. 2016; 6: 50.
- [25] Fan HC, Fu GK, Fodor SPA. Expression profiling. Combinatorial labeling of single cells for gene expression cytometry. *Science (New York, N.Y.)*. 2015; 347: 1258367.
- [26] Birey F, Andersen J, Makinson CD, Islam S, Wei W, Huber N, *et al.* Assembly of functionally integrated human forebrain spheroids. *Nature*. 2017; 545: 54–59.
- [27] Deng Q, Ramsköld D, Reinius B, Sandberg R. Single-cell RNA-seq reveals dynamic, random monoallelic gene expression in mammalian cells. *Science (New York, N.Y.)*. 2014; 343: 193–196.
- [28] Macosko EZ, Basu A, Satija R, Nemes J, Shekhar K, Goldman M, *et al.* Highly Parallel Genome-wide Expression Profiling of Individual Cells Using Nanoliter Droplets. *Cell*. 2015; 161: 1202–1214.
- [29] Shekhar K, Lapan SW, Whitney IE, Tran NM, Macosko EZ, Kowalczyk M, *et al.* Comprehensive Classification of Retinal Bipolar Neurons by Single-Cell Transcriptomics. *Cell*. 2016; 166: 1308–1323.e30.
- [30] Tasic B, Menon V, Nguyen TN, Kim TK, Jarsky T, Yao Z, *et al.* Adult mouse cortical cell taxonomy revealed by single cell transcriptomics. *Nature Neuroscience*. 2016; 19: 335–346.
- [31] Colonna M, Butovsky O. Microglia Function in the Central Nervous System During Health and Neurodegeneration. *Annual Review of Immunology*. 2017; 35: 441–468.

- [32] Rajan WD, Wojtas B, Gielniewski B, Gieryng A, Zawadzka M, Kaminska B. Dissecting functional phenotypes of microglia and macrophages in the rat brain after transient cerebral ischemia. *Glia*. 2019; 67: 232–245.
- [33] Al-Ahmady ZS, Jasim D, Ahmad SS, Wong R, Haley M, Coutts G, *et al.* Selective Liposomal Transport through Blood Brain Barrier Disruption in Ischemic Stroke Reveals Two Distinct Therapeutic Opportunities. *ACS Nano*. 2019; 13: 12470–12486.
- [34] Ma Y, Wang J, Wang Y, Yang GY. The biphasic function of microglia in ischemic stroke. *Progress in Neurobiology*. 2017; 157: 247–272.
- [35] Hu X, Leak RK, Shi Y, Suenaga J, Gao Y, Zheng P, *et al.* Microglial and macrophage polarization—new prospects for brain repair. *Nature Reviews. Neurology*. 2015; 11: 56–64.
- [36] Zanolini L, Boutouyrie P, Fatuzzo P, Granata A, Lentini P, Oztürk K, *et al.* Inflammation and Aortic Stiffness: An Individual Participant Data Meta-Analysis in Patients With Inflammatory Bowel Disease. *Journal of the American Heart Association*. 2017; 6: e007003.